

# Ga<sub>1-x</sub>Al<sub>x</sub>As nanostructures grown on the GaAs Surface by Ion Implantation

Sodikjanov J.Sh.

Andijan Machine-Building Institute

[jsodikjanov@mail.ru](mailto:jsodikjanov@mail.ru)

**Abstract:** The surface structure and electronic characteristics of nanocrystalline phases and 2-7-nm-thick Ga<sub>1-x</sub>Al<sub>x</sub>As films formed on the GaAs(111) surface by Al<sup>+</sup> ion implantation are investigated. The bandgap E<sub>g</sub> of the Ga<sub>0.5</sub>Al<sub>0.5</sub>As nanocrystalline surface phase 25-30 nm in size is determined to be 2.8-2.9 eV.

**Keywords:** morphology, ion implantation, electronic structure, nanocrystalline, properties.

## Introduction

To date, ternary epitaxial Al-Ga-As, In-Ga-As, and Ga-In-P layers formed on the GaAs surface are well understood. These structures are often used in microelectronic and optoelectronic devices [1-6]. Multilayer Ga<sub>1-x</sub>Al<sub>x</sub>As/GaAs structures generated using molecular beam epitaxy (MBE) are of particular interest because the crystal structures and lattice properties of the film and substrate will match. According to simulations in [7, 8], the tetragonal Ga<sub>1-x</sub>Al<sub>x</sub>Ga<sub>1-s</sub>As solid solution is an indirect-gap material at  $x \leq 0.40-0.45$  and a direct-gap material at  $x > 0.45$ . Thus, the optical, electrical, and other characteristics of epitaxial structures are affected by the value of  $x$ . MBE-grown semiconductor films are known to be homogenous starting at a thickness of 10-15 nm [1]. 5-10 nm for next-generation optoelectronic and nanoelectronic devices.

Previously [9-12], our group investigated the effect of ion bombardment with Ar<sup>+</sup>, Ba<sup>+</sup>, and Na<sup>+</sup> on the surface composition and structure of GaAs films. It was discovered that when exposed to high-dose bombardment by Ar<sup>+</sup> ions, the surface becomes enriched with Ga atoms, and when exposed to metal (Ba, Na) ions, it gets enriched with Ga atoms and atoms of the bombarding metals. Furthermore, the surface structure becomes disorganized. When heated to the optimum temperature, epitaxial nanocrystalline phases (at implantation doses  $D \leq 10^{15} \text{ cm}^{-2}$ ) and Ga<sub>1-x</sub>Me<sub>x</sub>As (Me stands for a metal) nanocrystalline films (at  $D \geq 10^{16} \text{ cm}^{-2}$ ) are formed. However, no equivalent studies of GaAs implanted by slow ions ( $E_0 \leq 5-10 \text{ keV}$ ) were conducted.

We investigate the composition and electrical structure of Ga<sub>1-x</sub>Al<sub>x</sub>As nanocrystals and films formed on the GaAs surface through Al<sup>+</sup> ion implantation and subsequent (laser + thermal) annealing in this work.

## Materials and methods

The test items were  $d = 500 \text{ nm}$  thick n- and p-GaAs(111) films. The films were bombarded with Al<sup>+</sup> ions with ion energies  $E_0$  ranging from 0.5 to 5.0 keV and irradiation dose  $D$  ranging from  $10^{14}$  to  $10^{17} \text{ cm}^{-2}$ .

Scanning electron microscopy (SEM), high-energy electron diffraction (HEED), Auger electron spectroscopy (AES), and UV photoelectron spectroscopy (UVPS) were used in the study. Furthermore, we calculated the energy dependencies of the secondary electron emission coefficient (SEEC). Layer-by-layer Auger analysis was used to get the atom depth profile. To do this, the sample's surface was sputtered (etched) by 3-keV Ar<sup>+</sup> ions incident at an angle of roughly 85° to the normal. The etch rate was changed within a range of (5 1)/min. UV photoelectron spectra were collected at photon energies of  $h\nu 10.8 \text{ eV}$ . As a UV photon source, a typical gas-discharge hydrogen lamp was used. A SUPRA-40 device was used to take SEM micrographs. See [11] for further information on the experimental procedure.

## Result and Discussion

SEM micrographs and HEED patterns (insets) of the as-grown GaAs(111) surface and Ga<sub>1-x</sub>Al<sub>x</sub>As films generated by heating to 850 K following implantation of Al<sup>+</sup> ions with  $E_0 = 1 \text{ keV}$  and  $D = 4 \times 10^{16} \text{ cm}^{-2}$  are shown in Figure 1. In the present example, Auger data show that  $x$  falls between the range of 0.45-0.50. As a result, the approximate composition of the resultant chemical is Ga<sub>0.5</sub>Al<sub>0.5</sub>As. The quantity of Al can be

reduced by raising the temperature. For example, the surface concentration of Al at 950 K was 15-20 at%, and the film's composition was  $\text{Ga}_{0.7}\text{Al}_{0.3}\text{As}$ . According to Fig. 1, the GaAs surface exhibits a flat microrelief. The  $\text{Ga}_{0.5}\text{Al}_{0.5}\text{As}$  nanofilm is made up of singlecrystalline nanoblocks with surface sizes  $d = 10\text{-}20\text{ nm}$ . Despite the fact that these blocks were produced epitaxially, the grain-boundary crystallographic orientations of several of them varied. As a result, concentric rings of individual diffraction spots, typical of textured films, show in the HEED patterns. We found that when ion-implanted GaAs is annealed by laser radiation with energy density  $W = 1.6\text{ J/cm}^2$  and then is rapidly heated to 900–950 K, a homogeneous epitaxial  $\text{Ga}_{0.5}\text{Al}_{0.5}\text{As}$  film grows on the GaAs surface. The atom distribution profile taken of this system suggests that the  $\text{Ga}_{0.5}\text{Al}_{0.5}\text{As}$  film is 3.5–4.0 nm thick, and the thickness of the transition layer, where the Al concentration monotonically drops from 25 at % to zero, equals 5–6 nm (Fig. 2).

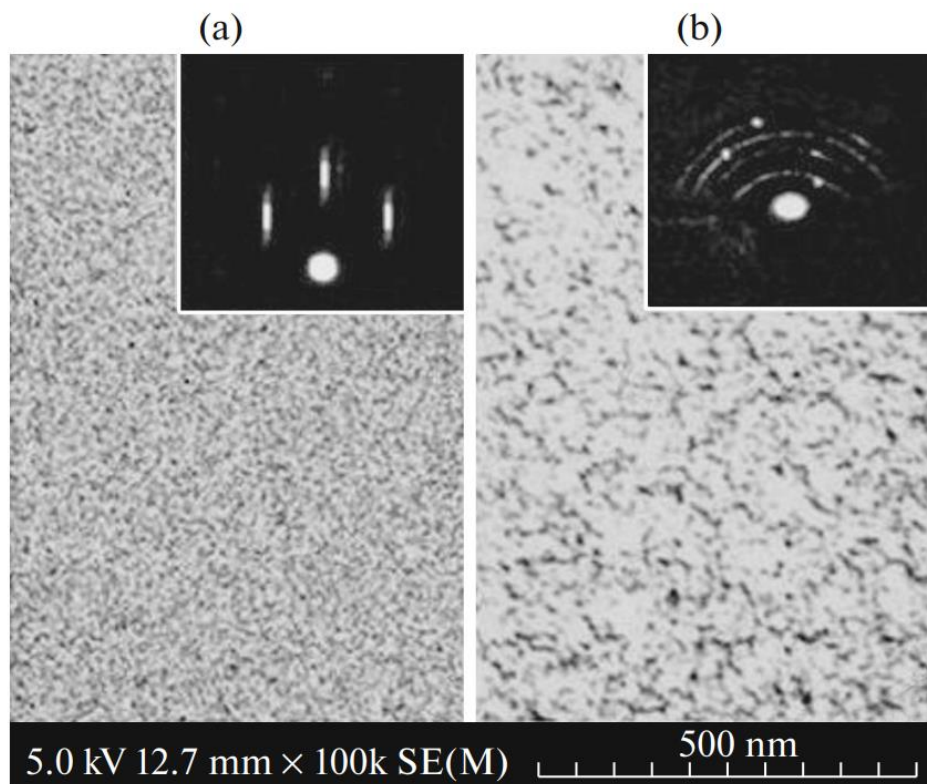


**Fig. 1.** SEM micrographs and HEED patterns of the surface of (a) GaAs(111) and (b)  $\text{Ga}_{0.5}\text{Al}_{0.5}\text{As}$  films formed by 1-keV  $\text{Al}^+$  ion implantation with a dosage of  $4 \times 10^{16}\text{ cm}^{-2}$  followed by heating are shown

The photoelectron spectra of GaAs and the  $\text{Ga}_{0.5}\text{Al}_{0.5}\text{As}$  film were recorded at photon energy of 10.8 keV in Figure 3. Four different peaks can be detected in the spectrum of GaAs, which are caused by the excitation of s-electrons in As and p-electrons in Ga and As. Additionally, surface state-related singularities are seen close to  $E_4$  as well. The following modifications occur because of ternary compound production.

- (i) Peak EV moves 0.3–0.4 eV farther from EB as the spectrum grows 0.3–0.4 eV narrower.
- (ii) Peak E1 broadens significantly and transitions toward higher energies. We believe that this peak was formed in part by the 4p-electrons of Ga and the 3p-electrons of Al.
- (iii) The magnitude of the Peak E2 caused by the splitting of the p-states in Ga, Al, and As moves to the right by 0.1–0.2 eV.

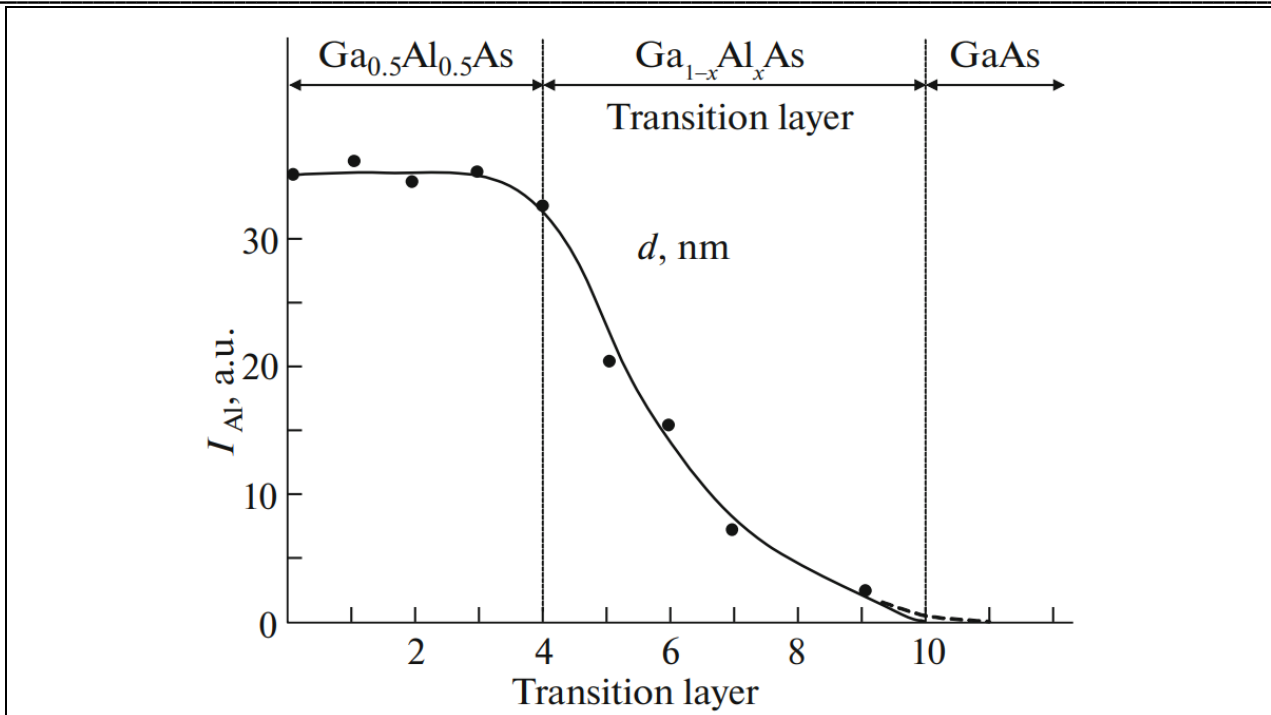


**Fig. 2.** The Ga<sub>0.5</sub>Al<sub>0.5</sub>As /GaAs system's depth profile was created via the implantation of 1-keV Al<sup>+</sup> ions with a dosage of 4×10<sup>16</sup> cm<sup>-2</sup> into GaAs, followed by (laser + thermal) annealing.

(iv) The only significant difference between the arsenic peaks E<sub>3</sub> and E<sub>4</sub> is a little shift in their intensities.

Ga<sub>0.5</sub>Al<sub>0.5</sub>As films with thicknesses between 2.0-2.5 and 6.0-7.0 nm may be grown by varying the energy of Al ions in the range of 0.5-5.0 keV. GaAs implanted with Al ions at energy E<sub>0</sub> = 1 keV and low dose (D = 8×10<sup>14</sup> cm<sup>-2</sup>) underwent (laser + thermal) annealing to form epitaxial nanocrystalline phases of the ternary Ga<sub>0.5</sub>Al<sub>0.5</sub>As compound, which, like Si [12], had surface diameter d = 15-20 nm. These phases' centers were separated by 50–60 nm. It is well known that the band diagrams of semiconductors and dielectrics coincide with the energy dependence of the SEEC measured in the energy range of 1–25 eV [13]. The (E<sub>p</sub>), R(E<sub>p</sub>), and (E<sub>p</sub>) curves for the Ga<sub>0.5</sub>Al<sub>0.5</sub>As /GaAs (111) nanofilms with thickness = 4 nm are shown in Figure 4. Here, R is the coefficient of elastically scattered electrons, is the total SEEC, is the coefficient of genuine secondary electrons, and is the total SEEC.

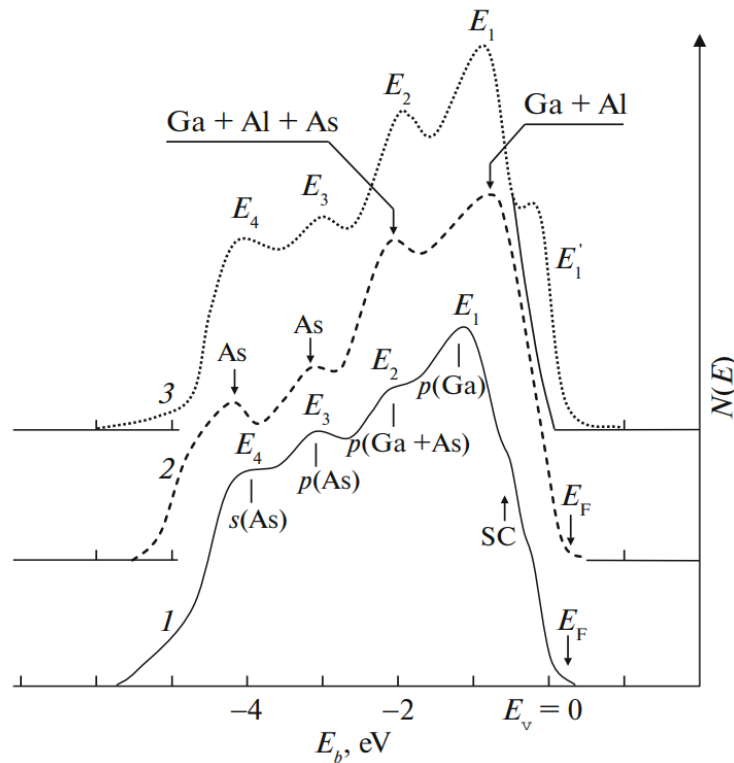


**Fig. 3.** Photoelectron spectra of three different films were obtained: (1) pure GaAs/Ge(111) film; (2) Ga<sub>0.5</sub>Al<sub>0.5</sub>As /GaAs(111) nanofilm; and (3) GaAs film containing Ga<sub>0.5</sub>Al<sub>0.5</sub>As nanocrystals that were 15-20 nm thick.

Figure 4 shows that the initial drop R is located between 2.0 and 2.1 eV. This decrease denotes the beginning of the inelastic scattering of electrons without their escape into the vacuum; in other words, electrons go from the top of the valence band to the bottom of the conduction band, or  $= E_g$ . When begins to increase, R experiences its second abrupt dip. Here, electron emission into a vacuum occurs, and the equation is  $E_g + \chi$ .

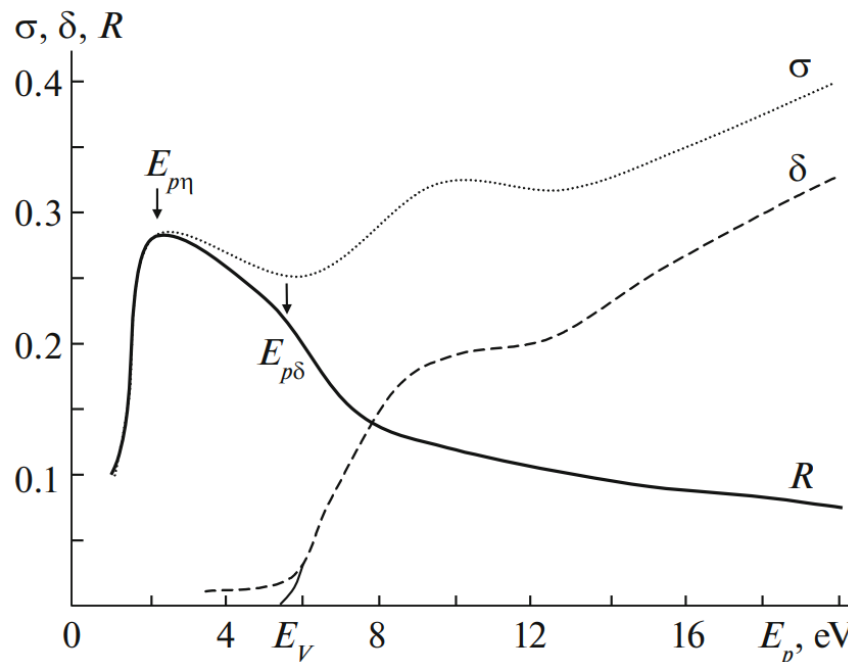


**Fig. 4.** ( $E_p$ ),  $R(E_p)$ , as well as ( $E_p$ ) profiles for the 4 nm thicker Ga<sub>0.5</sub>Al<sub>0.5</sub>As film

Thus, ion implantation combined with annealing is an effective way of producing ternary Ga<sub>1-x</sub>Al<sub>x</sub>As nanofilms and nanocrystals in the surface area GaAs with new electronic properties.

### Conclusion

Ternary Ga<sub>1-x</sub>Al<sub>x</sub>As nanostructures 2–7 nm thin were produced on the surface of a GaAs crystal by annealing after Al<sup>+</sup> ion implantation at energies ranging from 0.5 to 5.0 keV. Ga<sub>0.5</sub>Al<sub>0.5</sub>As nanofilms developed at higher doses ( $D \leq 2 \times 10^{16} \text{ cm}^{-2}$ ) whereas nanocrystalline phases developed at lower doses ( $D \geq 10^{15} \text{ cm}^{-2}$ ). One may change x in the range of 0.5-0.2 by varying the post-implantation annealing temperature between 850 and 1000 K. The films that were produced following a laser annealing and quick thermal heating were the most homogenous. E<sub>g</sub> was calculated to be around 2.3 eV for the 2.0–2.5 nm thick Ga<sub>0.5</sub>Al<sub>0.5</sub>As /GaAs nanofilm and 2.9 eV for the Ga<sub>0.5</sub>Al<sub>0.5</sub>As nanocrystal.

### References

1. L. L. Chang and K. Ploog, *Molecular Beam Epitaxy and Heterostructures* (Nijhoff, Boston, 1985).
2. V. V. Zolotarev, A. Yu. Leshko, A. V. Lyutetskii, D. N. Nikolaev, N. A. Pikhtin, et al., *Semiconductors* 47, 122 (2013).
3. D. A. Vinokurov, S. A. Zorina, V. A. Kapitonov, A. V. Murashova, D. N. Nikolaev, et al., *Semiconductors* 39, 370 (2005).
4. D. S. Abramkin, K. S. Zhuravlev, T. S. Shamirzaev, A. V. Nenashev, and A. K. Kalagin, *Semiconductors* 45, 179 (2011).
5. S. A. Vaganov and R. P. Seisyan, *Semiconductors* 39, 103 (2011).
6. P. V. Seregin, E. P. Domashevskaya, I. N. Arsent'ev, D. A. Vinokurov, A. L. Stankevich, and T. Prutskij, *Semiconductors* 47, 1 (2013).
7. S. Laref, S. Mec-abih, B. Abbar, B. Bouhafs, and A. Laref, *Physica B* 396, 169 (2007).
8. Su-Huai Wei and A. Zunger, *Phys. Rev. B* 39, 700 (1989).
9. J.Sh. Sodikjanov, B.E. Umirzakov, *Poverkhnost': Rentgen. Sinkhrotron. Neitron. Issled.*, No., 15, 263 (2021).
10. Kh. Kh. Boltaev, J.Sh. Sodikjanov, D. A. Tashmukhamedova, B. E. Umirzakov, *Tech. Phys.* 62, 1882 (2017).
11. B. E. Umirzakov, M. T. Normuradov, D. A. Tashmukhamedova, and A. K. Tashatov, *Nanomaterials and Perspectives of Their Application (MERIYUS, Tashkent, 2008)*.
12. Kh. Kh. Boltaev, D. A. Tashmukhamedova, and B. E. Umirzakov, *Poverkhnost': Rentgen. Sinkhrotron. Neitron. Issled.*, No. 4, 24 (2014).
13. S. A. Fridrikhov and S. M. Movin, *Physical Grounds of Electronic Engineering (Vysshaya Shkola, Moscow, 1982)*. Translated by V. Isaakya